Damascus University Journal of Earthquake and Disaster Research
Vo 3 number (1) -2026: 17-36

مجلة جامعة دمشق لبحوث الزلازل والكوارث
المجلد 3 العدد (1) – 2026: 17-36

Seismic Performance Modeling in Earth-Fill Dams with Geotechnical Anomalies: A Comparative Study of MCC and Mohr-Coulomb Approaches

Modar Tawfik Donia[*1] Ibrahim Diab Hammoud[2] Nedal Shareef Shouker[3]

*1. PHD student, Eng, Higher Institute for Earthquake Studies and Research, Damascus University. modar.donia@damascusuniversity.edu.sy

2 Professor, Geotechnical Engineering Department –Faculty of Civil Engineering-Damascus University..

abdulmunir. Najem@damascusuniversity.edu.sy

3. Professor, Geology, Higher Institute for Earthquake Studies and Research, Damascus University. nedal.shouker@damascusuniversity.edu.sy

Received: 30/7/2025
Accepted: 15/3/2026

Abstract:

This study presents a seismic analysis that includes comprehensive geotechnical and numerical assessment of aging earth-fill dams (Al-Moshanaf earth-fill dam) in southern Syria where expansive clay soils is widespread, that dam has experienced upstream slope failure in recent years. Field sampling and laboratory testing were conducted to evaluate soil variability across dam zones, revealing significant heterogeneity in consolidation and swelling behavior. Using field investigations, lab tests, and simulation techniques, the study characterizes compressibility behavior, variations in moisture content, unit weight and specific gravity in geotechnical anomalies zones across the dam. Twelve representative samples underwent consolidation testing (ASTM D4546) and (ASTM D2435), showing variability in compression indices (Cc = 0.23–0.37) and swelling ratios (Cs/Cc = 5–56%), between samples located directly under upstream face and samples from inside dam body at the same level, exhibiting significant fine particles loss and lower moisture content due to long-term exposure and seepage-induced suffusion. To simulate the dam's response under different loading conditions, advanced numerical modeling using FLAC3D v6 was performed, employing both Mohr-Coulomb and Modified Cam-Clay (MCC) constitutive models. Interface elements were introduced to simulate inter-zonal discontinuities. Static analysis under gravity and reservoir loading revealed that zones with high compressibility and swelling index ratios underwent substantial displacements. Results revealed settlements up to 14.4 cm under gravity and reservoir loads, with effective stress reductions up to 62% when pore pressure effects were included. Dynamic simulations under seismic loading showed, that in the case of applying elastic constitutive model, dam failure occurs after 5 sec and acceleration is amplified 42 times at dam crest, while in the case MCC model, failure occurs after 1.88 sec and acceleration is amplified 3.7 times at the crest which. by comparing both cases, elastic constitutive model analysis showed maximum displacements toward downstream, and at dam crest 3.5m, toe 7.8m, while at dam heel displacements were toward upstream by 0.8m. in the case of MCC model, displacements occur in toward downstream, and at dam crest 0.65m, toe 1.2m, while at dam heel the maximum displacements occur toward upstream by 32m, which is the more realistic results taking into consideration static analysis and actual field conditions. as a result, the MCC model better replicated the observed deformation behavior, including plastic displacements and collapse, supported by laboratory-derived parameters. This study demonstrates that spatially resolved material zoning improves predictive accuracy, validates the use of MCC for seismic analysis in heterogeneous dam structures, and establishes a reliable methodological foundation for future dynamic safety evaluations.

Keywords: Earth-fill dam, Geotechnical anomalies, Consolidation tests, Comparative analysis, Cyclic wetting, Mohr-coulomb, Modified Cam-Clay, finite difference method.

ISSN (online): 3031-085X

نمذجة الأداء الزلزالي في السدود الترابية ذات عدم الانتظام الجيوتكنيكي: دراسة مقارنة بين نموذجي السلوك اللاخطي–كام كلاي المعدل، والسلوك الخطي– موهر–كولومب

مضر توفيق دنيا[*1] عبد المنير خليل نجم[2] نضال شريف شقير[3]

*1. طالب دكتوراه، مهندس في قسم الهندسة الجيوتكنيكية الزازالية، المعهد العالي للبحوث والدراسات الزلزالية، جامعة دمشق.
modar.donia@damascusuniversity.edu.sy

2. دكتور، مهندس، أستاذ في قسم الهندسة الجيوتكنيكية، كلية الهندسة المدنية، جامعة دمشق.
abdulmunir. Najem@damascusuniversity.edu.sy

3. دكتور، أستاذ مساعد في قسم الجيولوجيا، المعهد العالي للبحوث والدراسات الزلزالية، جامعة دمشق.
nedal.shouker@damascusuniversity.edu.sy

الملخص:

يتأثر يقدم البحث دراسة تحليلية تقييما شاملا جيوتكنيكيا وعدديا لسد ترابي قديم الانشاء (سد المشنف الشمالي)، يقع في المنطقة الجنوبية من سوريا التي تتميز بانتشار الترب الغضارية الانتفاخية، وقد تعرض السد في السنوات الأخيرة لانهيار على الوجه الأمامي للسد. تم أخذ عينات حقلية وتنفيذ تجارب مخبرية لتقييم التباينات في الخصائص الجيوتكنيكية لمادة انشاء جسم السد، حيث بينت التجارب وجود عدم تجانس في سلوك الانضغاطية والانتفاخ. باستخدام نتائج التحريات الحقلية والمخبرية وتقنيات المحاكات الرقمية، تناول البحث سلوك الانضغاطية، التغيرات في رطوبة التربة، الوزن الحجمي، الوزن النوعي في المناطق غير المتجانسة داخل جسم السد. تم اجراء تجارب الانضغاطية على 12 عينة تمثل المناطق المختلفة بحسب المواصفة ASTM D4546، والمواصفة ASTM D2435, حيث بينت النتائج تباينات في قرائن الانضغاطية ونسب الانتفاخ بين العينات المأخوذة من العينات الواقعة مباشرة تحت الوجه الأمامي للسد مقارنة بالعينات من داخل جسم السد المتموضعة على نفس المنسوب، إضافة لانخفاض في رطوبة العينات نتيجة لتفريغ السد لزمن طويل ولهروب الذرات الناعمة من هذه المناطق بسبب الشروحات . لتحليل استجابة السد عند تعرضه لمختلف حالات التحميل، تم بناء نموذج رقمي باستخدام (FLAC3D v6) وباستخدام كلا من نموذجي سلوك موهر كولومب وكام كلاي المعدل. تمت نمذجة السطوح البينية للفصل بين المناطق المتباينة داخل جسم السد. بين التحليل الستاتيكي نتيجة الحمولات الذاتية وحمولة ضغط ماء البحيرة على الوجه الامامي للسد، ان المناطق التي تتصف بالارتفاع النسبي لقرائن الانضغاطية والانتفاخ قد تعرضت لانتقالات كبيرة. وبين التحليل حدوث زيادة في الهبوطات وانخفاض في الاجهادات الفعالة بتأثير ضغط الماء المسامي. بين التحليل الديناميكي بتأثير الحمولات الزلزالية انه وفي حالة اعتماد نموذج سلوك موهر كولومب (السلوك الخطي)، يحدث انهيار السد بعد 5 ثواني من تطبيق الحمولة الزلزالية حيث يحدث تضخيم للتسارع الزلزالي بمقدار 42 مرة على قمة السد مقارنة بالتسارع الزلزالي المطبق، أما في حالة اعتماد نموذج سلوك المادة كام كلاي المعدل، يحدث انهيار السد بعد 1.88 ثانية ويحدث تضخيم للتسارع الزلزالي في نفس المكان بمقدار 3.7 مرة. وبمقارنة الانتقالات يتبين انه في حالة السلوك الخطي تكون الانتقالات الاعظمية باتجاه الوجه الخلفي عند قمة السد، وباتجاه القدم الخلفية بينما تبقى انتقالات القدم الامامية محدودة باتجاه الوجه الأمامي. أما في حالة اعتماد نموذج كام كلاي المعدل (السلوك اللاخطي)، تكون الانتقالات محدودة باتجاه الوجه الخلفي عند قمة السد، وباتجاه القدم الخلفية بينما تكون الانتقالات الأعظمية عند القدم الامامية باتجاه الوجه الأمامي. وهو السلوك الأكثر واقعية بالأخذ بالاعتبار نتائج التحليل الستاتيكي والظروف الحقيقية الحقلية. بناء عليه يعتبر سلوك المادة اللاخطي هو الأفضل لتمثيل سلوك التشوهات في السد، والانتقالات اللدنة والانهيار بما يتوافق مع نتائج التجارب المخبرية. يبين هذا البحث أن تحليل السد بالأخذ بالاعتبار التباينات الجيوتكنيكية للمناطق في جسم السد يحقق تحليلا أكثر دقة وتنبأ أفضل بسلوك السد مما يحقق قاعدة منهجية لزيادة موثوقية التقييم الزلزالي للسدود.

الكلمات المفتاحية: السدود الترابية، عدم الانتظام الجيوتكنيكي، انضغاطية التربة، تجارب الانضغاطية، دراسة مقارنة، تأثير الترطيب الدوري للتربة. نموذج Mohr-coulomb. نموذج Cam-Clay. طريقة الفروقات المحدودة.

تاريخ الايداع: 2025/7/30

تاريخ القبول: 2026/3/15

Introduction:

Earth-fill dams play a critical role in water retention, flood protection, and irrigation systems. Their long-term performance, however, is often compromised by geotechnical irregularities, including heterogeneous soil properties, material interfaces, and consolidation-induced deformations. The Al-Moshanaf Dam, located in southern Syria, has shown signs of structural distress, including upstream slope instability. Understanding the root causes of these deformations requires an integrated approach that combines experimental characterization with advanced numerical modelling techniques. This study builds on previous laboratory investigations by incorporating static and dynamic numerical analyses using FLAC3D v6 to simulate the dam's behaviour under gravity, reservoir, and seismic loading. The application of both the Mohr-Coulomb and Modified Cam-Clay models enables a comparative assessment of linear versus nonlinear soil behaviour in capturing real-world deformation mechanisms.

1. Experimental Assessment:

Twelve specimens were systematically extracted from boreholes located along the dam's longitudinal axis, spanning the crest, upstream face, and downstream face. The geotechnical parameters derived from these samples would be assigned to corresponding irregular zones within the dam model by cross-referencing their positions with the dam's cross-sectional layout. This spatial correlation enabled a comparative analysis with historical records of dam material properties, highlighting variability in soil composition attributable to environmental exposure and hydraulic influences. The results of these laboratory investigations provide a foundation for assessing material compatibility in dam evaluation and rehabilitation efforts. A comprehensive series of laboratory tests was conducted on soil samples extracted from multiple sections of dam embankments in southern Syria, focusing on moisture content, density variations, grain size distribution, Atterberg limits, and compressibility characteristics. Consolidation tests. To ensure comparative analysis, newly extracted samples were systematically compared to historical records of dam material properties, highlighting variability in soil composition due to environmental exposure and hydraulic influences. The findings from these laboratory investigations serve as a foundation for understanding material compatibility in dam evaluation and rehabilitation efforts. A comparison of the moisture content of old and new samples revealed a significant reduction in the moisture of recently collected samples due to the dam drawdown between 2018 (immediately after the slip occurred on the front face) and 2024 (when the new samples were taken), Fig.1. A comparison of the bulk natural density of new and old samples reveals an increase in the bulk density of the new samples, with average variations not exceeding 6%, Fig.2 A comparison of the specific gravity of new and old samples, Fig.3, indicates a reduction in the specific gravity of the new samples compared to the old ones, with the largest decrease (23%) observed in sample 2-2 located at the upstream toe of the dam.

In general, newly extracted soil samples exhibited lower specific gravity values compared to historical records, indicating material degradation and particle loss, particularly within zones exposed to seepage, Horikoshi et al [26].

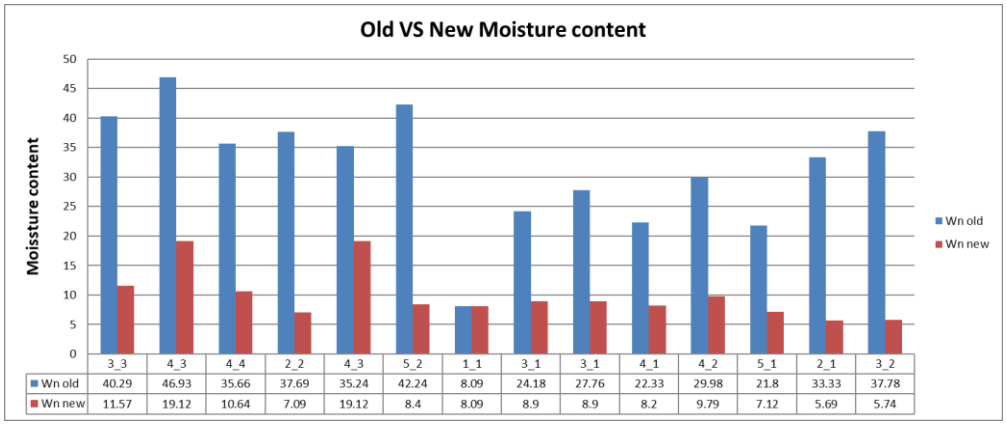

	3_3	4_3	4_4	2_2	4_3	5_2	1_1	3_1	3_1	4_1	4_2	5_1	2_1	3_2
Wn old	40.29	46.93	35.66	37.69	35.24	42.24	8.09	24.18	27.76	22.33	29.98	21.8	33.33	37.78
Wn new	11.57	19.12	10.64	7.09	19.12	8.4	8.09	8.9	8.9	8.2	9.79	7.12	5.69	5.74

Fig (1) comparison of the moisture content of old and new samples.

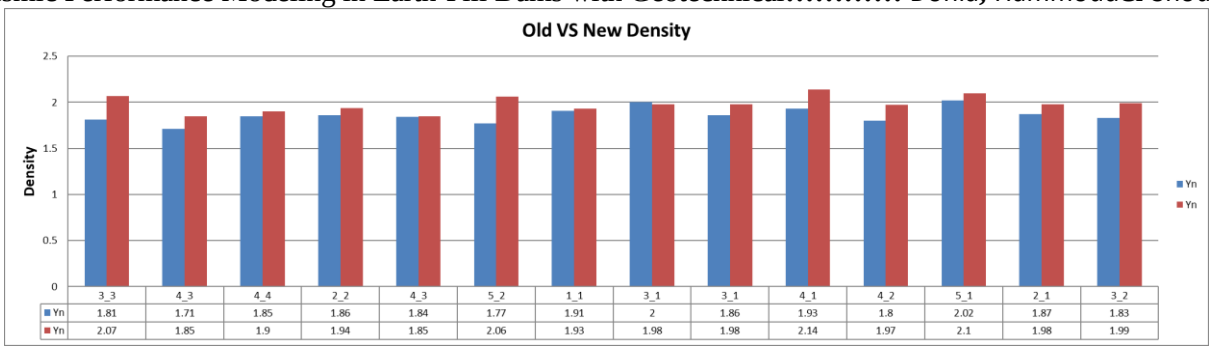

	3_3	4_3	4_4	2_2	4_3	5_2	1_1	3_1	3_1	4_1	4_2	5_1	2_1	3_2
Yn	1.81	1.71	1.85	1.86	1.84	1.77	1.91	2	1.86	1.93	1.8	2.02	1.87	1.83
Yn	2.07	1.85	1.9	1.94	1.85	2.06	1.93	1.98	1.98	2.14	1.97	2.1	1.98	1.99

Fig(2) comparison of the bulk natural density of new and old samples.

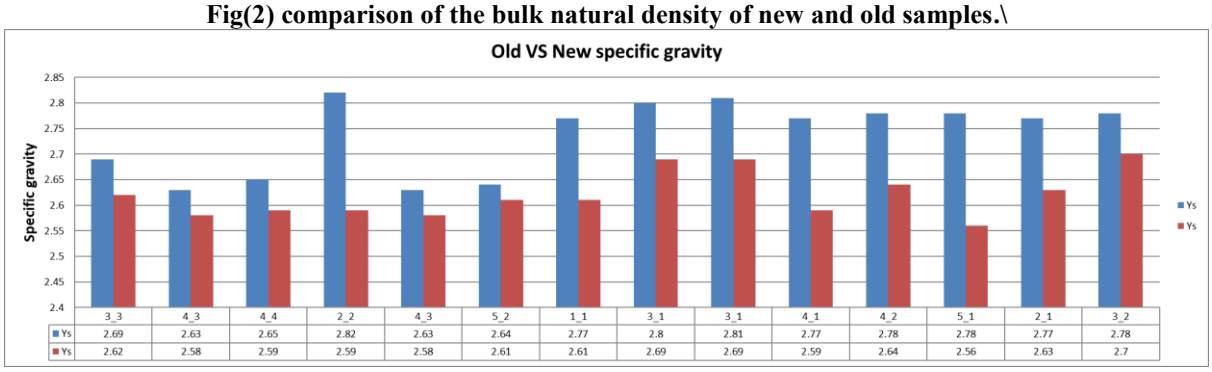

	3_3	4_3	4_4	2_2	4_3	5_2	1_1	3_1	3_1	4_1	4_2	5_1	2_1	3_2
Ys	2.69	2.63	2.65	2.82	2.63	2.64	2.77	2.8	2.81	2.77	2.78	2.78	2.77	2.78
Ys	2.62	2.58	2.59	2.59	2.58	2.61	2.61	2.69	2.69	2.59	2.64	2.56	2.63	2.7

Fig(3) comparison of the specific gravity of new and old samples

Consolidation tests conducted on embankment soil samples provided critical insights into settlement trends, compressibility behaviour, and structural stability of earth-fill dams. Using ASTM D2435 (standard one-dimensional consolidation test) and ASTM D4546 (evaluation of wetting-induced volume change), the study quantified swelling tendencies, compression indices, and differential expansion effects across embankment zones. ASTM D4546-14 is particularly relevant for evaluating the behaviour of earth-fill dams under wetting-induced deformation. In this test, specimens are examined in their natural moisture state and subjected to gradual loading equivalent to the overburden pressure of the soil column above them. Following this, they are inundated, simulating the first filling of a dam reservoir.

The loading-unloading cycle during the initial phase replicates the response of the soil structure to first reservoir filling, while the subsequent cycle mimics second reservoir filling, ensuring the test conditions closely resemble real-world site behaviour. Consequently, all consolidation tests are conducted in accordance with ASTM D4546-14. The greater compression, occurs during the first loading cycle corresponding to the initial filling and drawdown phase of the dam (i.e., the highest compression and thus the largest settlement would occur during the first filling), a comparison of the swelling-compression ratio (Cs/Cc) between the first and second loading cycles (corresponding to the second phase of filling and drawdown) , Fig .4, indicates that repeating the second cycle of filling and drawdown would induce greater relative compression and swelling. This would result in an increased probability of crack initiation and propagation over time, Guo et al [25].

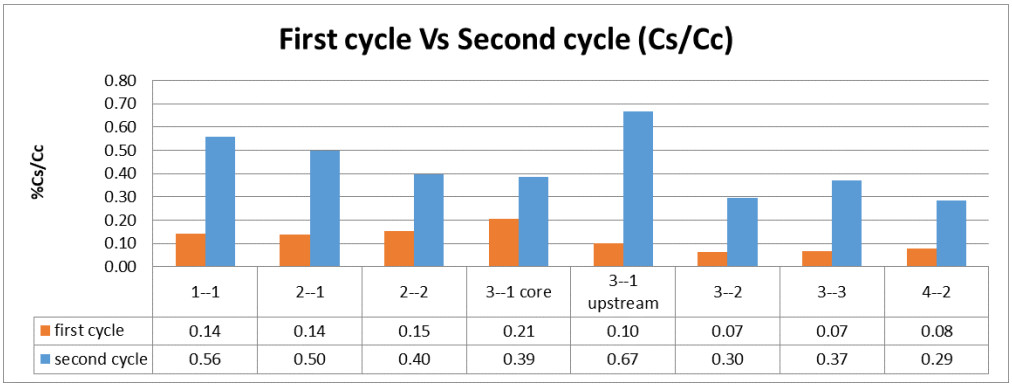

Fig (4) comparison of the swelling-compression ratio (Cs/Cc) between the first and second loading cycles

The most significant variation is observed in samples (1-1) and (3-1 upstream): for sample (1-1) during the first loading cycle, the swelling-to-compression ratio is 14% of the compression ratio, whereas it rises to 56% in the second loading cycle. for sample (3-1 upstream) during the first loading cycle, the swelling-to-compression ratio is 10% of the compression ratio, whereas it rises to 67% in the second loading cycle, Fig. 4. comparison of the compression and swelling indexes (Cc, Cs) between the first and second loading cycles are demonstrated in Fig.5 and Fig.6.

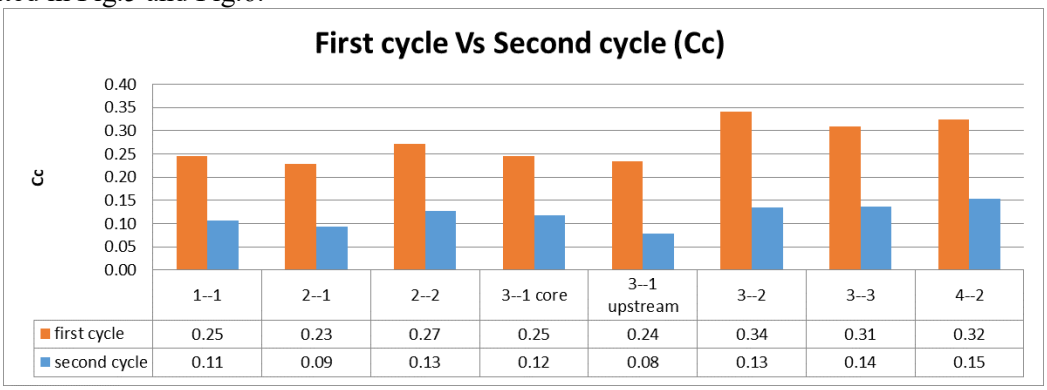

Fig (5) comparison of the compression index (Cc) between the first and second loading cycles.

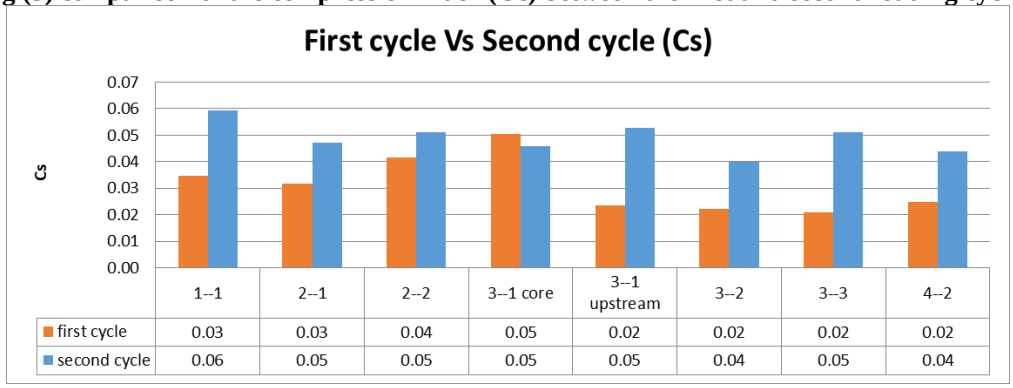

Fig (6) comparison of the swelling index (Cs) between the first and second loading cycles.

To achieve a clearer understanding of the relationship between the compressibility characteristics of representative samples from different zones within the dam body and how these characteristics influence their mutual behaviour, the locations of these samples in the dam body were correlated with their compressibility

http://journal.damascusuniversity.edu.sy/index.php/index/index

ISSN (online): 3031-085X

properties and the crack previously observed on the upstream face of the dam. A comparison of the results from the first set of oedometer tests reveals a correlation between samples (2-1) and (2-2), located on the same cross-sectional plane at the initiation of the slip surface, Fig .7.

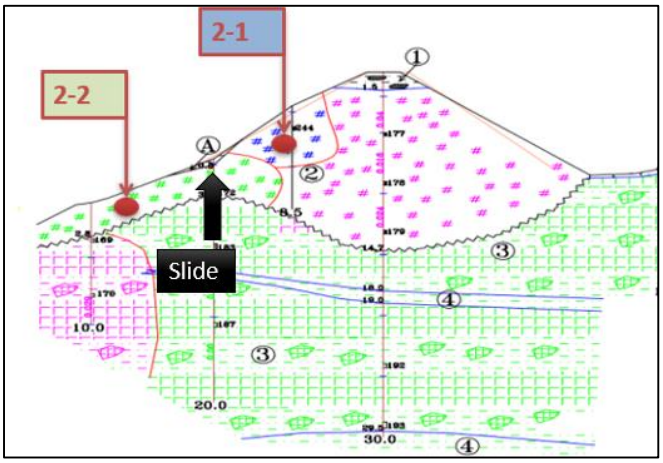

Fig (7) location of samples 2-1 and 2-2

Comparing the swelling percentage during saturation (first reservoir filling) shows that the swelling percentage in zone (2-1) is (0.15%), that is lower than that in zone (2-2) (1.5%), Fig .8. Furthermore, comparing the compression index (Cc) values between the first loading cycle (initial filling), of samples (Cc 2-1 = 0.23) and (Cc 2-2 = 0.27), and the second loading cycle (Cc 2-1 = 0.09) and (Cc 2-2 = 0.13) , Fig .5, demonstrates that the compressibility of the zone represented by sample (2-2) is higher than that of the overlying zone, This explains the development of the slip surface at the interface between these two zones, Fig .7.

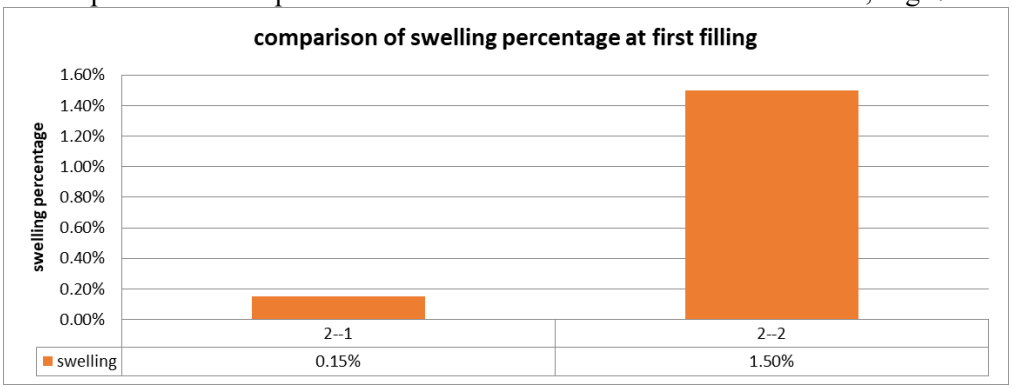

Fig (8) comparison of the swelling percentage between samples 2-1 and 2-2.

A comparison of the results from the first set of oedometer tests establishes a correlation between samples (3-1), (3-2), and (3-3), situated on the same cross-sectional plane at the slip surface, Fig .9. Analysis of the swelling percentage during saturation (initial reservoir filling) indicates that the swelling percentage in zone (3-1) is (0.2%), while zones (3-2) and (3-3) exhibit deformation in the compression direction, Fig .10, that is correlated with higher value of swelling index of zone (3-1), Fig. 6. Furthermore, comparing the compression index (Cc) values between the first loading cycle (initial filling), of samples (Cc 3-1 =0.245), (Cc 3-2 =0.342) and (Cc 3-3 =0.31), and the second loading cycle, of samples (Cc 3-1 =0.118), (Cc 3-2 =0.135) and (Cc 3-3 =0.137), Fig .5, reveals that the compressibility of the zone represented by sample (3-1) is lower than that of zones (3-2) and (3-3). This differential compressibility explains the formation of the slip surface at the interface between these zones.

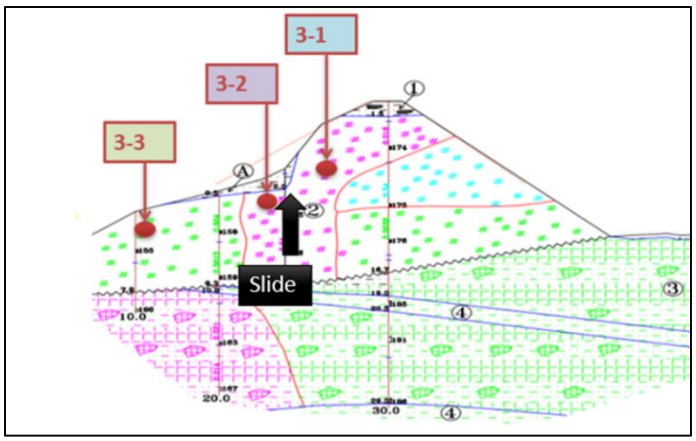

Fig (9) location of samples 3-1, 3-2 and 3-3.

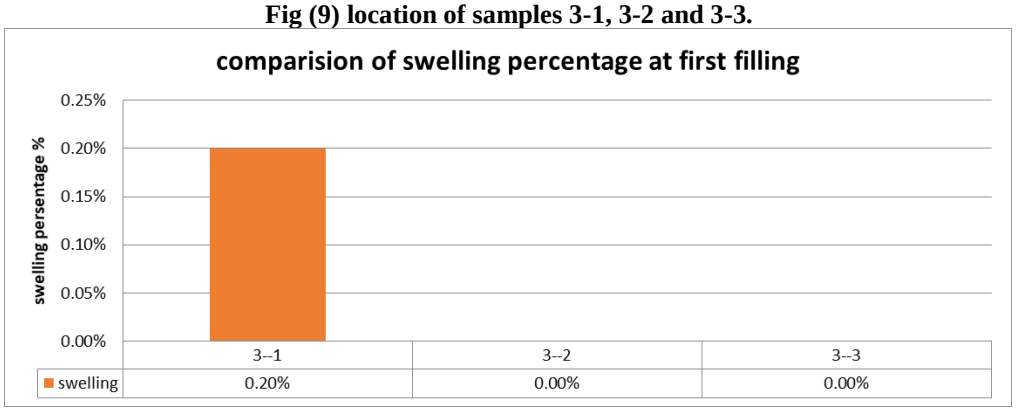

Fig (10) comparison of the swelling percentage between samples 3-1, 3-2 and 3-3.

In addition to variations in the geotechnical properties of samples based on the zone they represent; the spatial variability of these samples significantly influences their swelling and compressibility behaviour. This is reflected in parameters such as the indexes of compressibility and swelling. The most pronounced changes occur in samples extracted from upstream face of the dam, Fig .11, amplifying inconsistencies in swelling behaviour between adjacent zones and even within a single zone

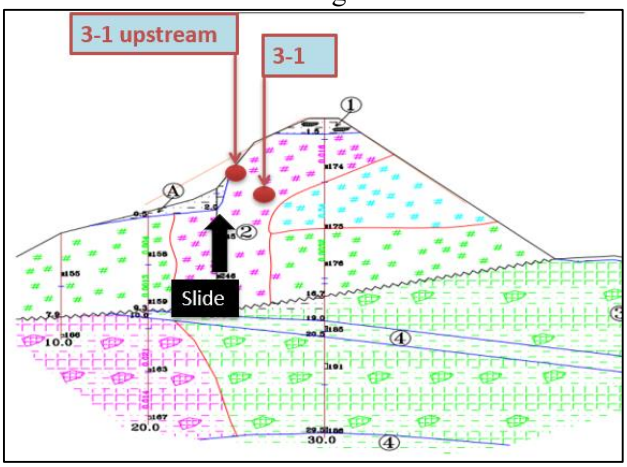

http://journal.damascusuniversity.edu.sy/index.php/index/index

ISSN (online): 3031-085X

Fig (11) location of samples (3-1) and (3-1 upstream).

The consolidation test results, demonstrates that the sample corresponding to the upstream soil undergoes the swelling percentage during saturation (first reservoir filling) shows that the swelling percentage in zone (3-1 core) is (0.2%), that is lower than that in zone (3-1 upstream) (0.3%). Furthermore, comparing the compression index (Cc) values between the first loading cycle (initial filling), of under-crest sample (Cc 3-1 core =0.25) and upstream sample (Cc 3-1 upstream =0.24), and the second loading cycle (Cc 3-1 core =0.12) and (Cc 3-1 upstream =0.08), demonstrates that the compressibility of the zone represented by sample (Cc 3-1 core) is higher than that of the adjusting zone (Cc 3-1 upstream), Fig .5. A comparison of the swelling index (Cs) for the two samples, reveals that during the first loading cycle, (Cs 3-1 core =0.03) and upstream sample (Cs 3-1 upstream =0.02), and the second loading cycle (Cs 3-1 core =0.049) and (Cs 3-1 upstream =0.053). This indicates that the spatial positioning of the samples (and consequently the applied weight of the overlying soil weight) leads to distinct mechanical behaviour during the initial filling-drawdown phase and the second filling-drawdown phase, Fig .6. Consolidation tests, revealed adaptation of swelling potential over multiple wetting cycles, demonstrating that initial inundation exerts greater influence than later saturation events, which emphasized nonlinear response in the zones of dam, illustrating how repeated saturation events influence soil stabilization rates, a factor that is critical for predicting long-term dam performance.

2. Numerical Analysis:

The three-dimensional model was constructed using FLAC-3D software by generating it from one of the cross-sections of the dam. FLAC3D (Fast Lagrangian Analysis of Continua in 3 Dimensions) Version 6 is a three-dimensional finite difference program designed for advanced geotechnical analysis. It excels at modeling the nonlinear, large-strain behavior of soils, rock, and other geomaterials. The program discretizes the model into volumetric zones. Internally, these zones are subdivided into tetrahedra for numerical calculation.

FLAC3D supports several zone types for building complex geometries: Brick (Hexahedral): Eight-node elements ideal for structured volumes like dam cores. Wedge: Six-node prismatic elements useful for transitions and slopes. Tetrahedral: Four-node elements for conforming to highly irregular shapes. Pyramid: Five-node transitional elements. Mesh Sizing requires balancing accuracy and computational speed. A finer mesh is essential in areas of high stress gradients (e.g., dam cores, interfaces) to capture behavior accurately, while a coarser mesh can be used in areas of low interest (e.g., far-field foundation).

A common practice is to use a graded mesh, refining it in critical zones and coarsening it elsewhere. The numerical model considers the variations in geotechnical properties of the zones the dam, as well as the changes in foundation elevations and the contact surface between the dam base and the foundation interface, Pardoen et al [9]. Each zone in dam body is related to geotechnical properties of the corresponding specimen, Fig .12.

The three-dimensional model was exported to FLAC3D V6 and processed using the FISH programming language. For the first model that represent the dam as one material, geotechnical properties were derived from the statistical analysis of field and laboratory data and were classified into three zones: the dam body, the rock foundation layer directly beneath the dam body, and the remaining rock foundation strata, Table.1.

The second model represent variation in dam zones according to laboratory tests. Initial constitutive behavior laws were assigned within the analytical models corresponding to each zone, to account for the variability in compressibility characteristics across different zones of the dam structure within static analysis, stiffness values (K) and shear modulus (G) were computed for each zone under the assumption of linear elastic behavior. This approach requires the evaluation of several parameters, most notably the coefficient of volume compressibility ($M\,v$) and the constrained modulus (D), both of which are critical for defining the elastic response of geomaterials, Hardin et al [29].

The methodology is considered suitable for representing compressibility effects within a framework based on the Mohr-Coulomb constitutive model, particularly when direct incorporation of nonlinear consolidation behavior is not feasible. All geotechnical properties are mentioned in Table.2.

The Mohr-Coulomb failure criterion is a widely used linear elastic-perfectly plastic model to represent the shear strength and failure behavior of soils and rock-like materials. Its primary function is to define a yield envelope beyond which the material undergoes irreversible plastic deformation. The failure condition is governed by the following relationship between the major (σ1) and minor (σ3) principal stresses at failure:

$$\sigma_1 = \sigma_3 \frac{1+\sin\phi}{1-\sin\phi} + 2c\frac{\cos\phi}{1-\sin\phi}$$

Where:

- c is the cohesion of the material, representing its inherent shear strength under zero confining pressure.
- ϕ is the angle of internal friction, defining the increase in shear strength with increasing normal stress.

In terms of shear stress (τ) and normal stress (σ_n) on a failure plane, the criterion can be expressed as:

$$\tau = c + \sigma_n \tan\phi$$

Within the FLAC3D simulation, prior to reaching this yield envelope, the material deforms elastically according to the defined shear modulus (G) and bulk modulus (K) derived from the compressibility parameters. Once the stress state satisfies the Mohr-Coulomb failure criterion, plastic strains develop, and the stress state is projected back onto the yield surface, simulating plastic flow and permanent deformation.
This model, while not capturing complex nonlinearities such as hardening or post-peak softening, provides a robust and computationally efficient framework for assessing the onset of yield and the general stability of geotechnical structures like dams under static loading conditions.

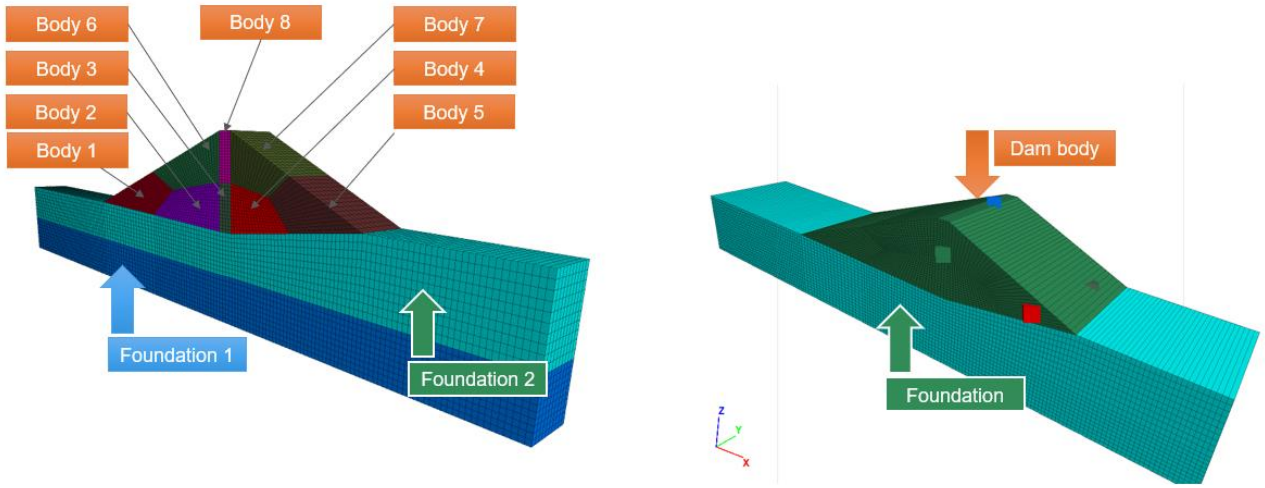

Fig (12) Three-dimensional models, homogeneous dam, and dam with anomalies (varying geotechnical Properties).

Table (1) Materials properties for homogenous dam and foundations.

No	Group-region	Cohesion (Kpa)	Friction (degree)	Density (t/m3)	Stiffness K=E/3*(1-2v)	Max shear modulus G=E/2*(1+v)	Constitutive model
1	Body	67	28	1.88	2.3e7	5e6	mohr-coulomb
2	Foundation	-	-	1.94	1e9	5e8	elastic
3	Left abutment	-	-	1.94	1e9	5e8	elastic
4	Right abutment	-	-	1.94	1e9	5e8	elastic

Table (2) Materials properties for dam body with anomalies.

	First cycle				Second Cycle			
TEST	D	Mv	K	G	D	Mv	K	G
1--1	8370.33	0.00012	4185.16	3138.87	18067.5	5.5E-05	9033.74	6775.3
1--2	8370.33	0.00012	4185.16	3138.87	20325.9	4.9E-05	10163	7622.21
2--2	7200.18	0.00014	3600.09	2700.07	13373.6	7.5E-05	6686.82	5015.12
3--1 modified	8955.76	0.00011	4477.88	3358.41	18578.5	5.4E-05	9289.27	6966.95
3--1 upstream	7033.91	0.00014	3516.95	2637.72	21500.9	4.7E-05	10750.4	8062.83
3--2	6516.93	0.00015	3258.46	2443.85	18060.8	5.5E-05	9030.42	6772.81
3--3	6578.04	0.00015	3289.02	2466.77	16066.1	6.2E-05	8033.04	6024.78
4--2	7126.21	0.00014	3563.11	2672.33	14689	6.8E-05	7344.5	5508.37

Comparison of Stress and Displacement Responses under Static Loading Conditions:

This analysis evaluates the impact of self-weight and hydrostatic loads induced by the reservoir on the dam structure under static conditions. The study includes a comparative assessment of stress distribution and displacement patterns for two dam section configurations: A homogeneous cross-section characterized by uniform geotechnical properties. A stratified or heterogeneous cross-section exhibiting spatially varying geotechnical specifications. The aim is to quantify how geometric and material discontinuities influence the dam's static response to gravitational and water-induced loading, providing insight into deformation behaviour and internal stress evolution across both design scenarios. Boundary conditions were imposed at the base of the model to restrict horizontal movement, while permitting vertical displacement along the remaining peripheral surfaces. The simulation revealed vertical settlements distributed along the dam axis, with maximum displacement occurring at the upper portion of the dam—directly beneath the crest on the upstream (water-facing) side—and in cross-sections exhibiting the greatest height. In case of dam's model with varying properties, the recorded settlements reached magnitudes up to 14.4 cm at upstream face and 8.4 cm at downstream face, while in case of dam's model with homogenous section, the recorded settlements reached

magnitudes up to 6.8 cm at upstream face and 5 cm at downstream face, Fig .13. accompanied by an increase in vertical stress in case of dam's model with varying properties, with peak values up to 500×10^3 Pa comparing to 92×10^3 Pa in case of dam's model with homogenous, Fig .14. Notably, these settlements and stresses spatially conform with the onset of sliding observed on the upstream face of the dam.

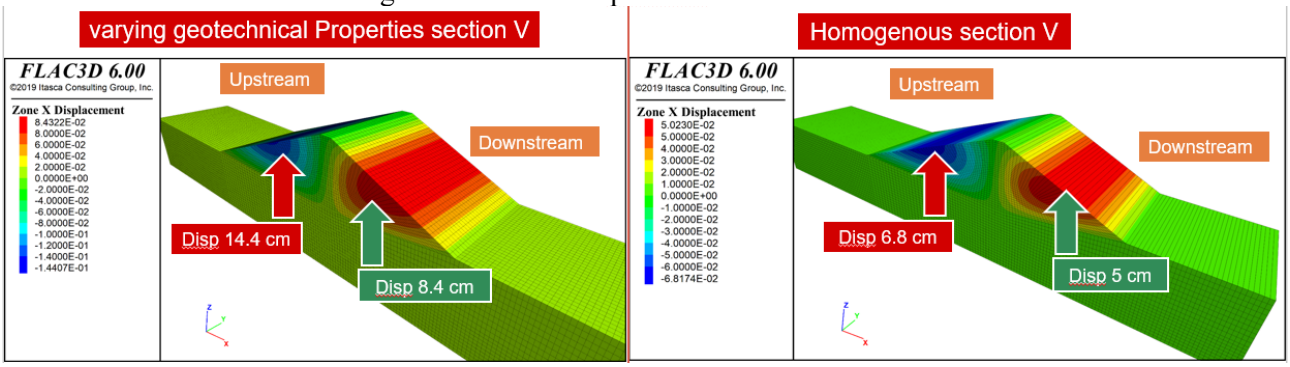

Fig. 13 vertical settlements distributed along the dam axis in both models.

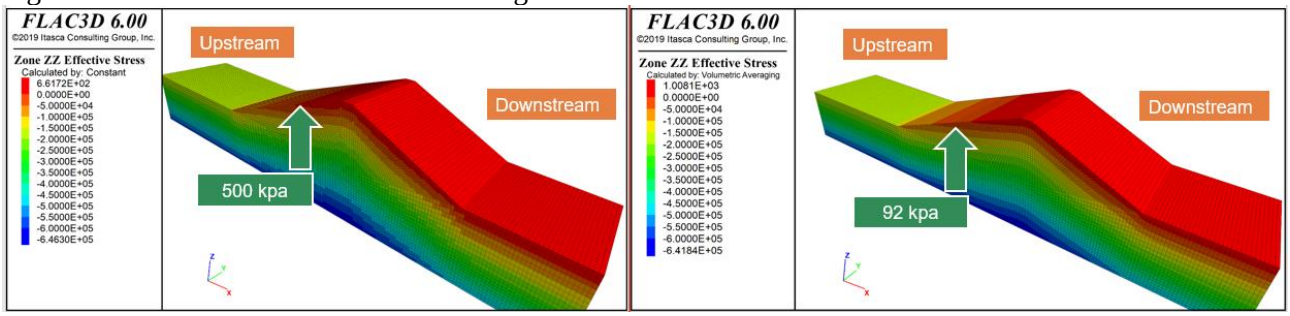

Fig (13) maximum vertical stresses under upstream face, in both models.

Comparison of Steady-State Seepage Analysis for both Models:

Seepage behavior within the dam body and its foundation layers was analyzed under steady-state flow conditions. Differential hydraulic conductivity values were assigned to the foundation strata, with distinct permeability characteristics specified for the upper 10-meter zone beneath the dam, based on results from in-situ permeability tests, Table.3. These tests indicated the presence of fissures in this layer, whereas deeper strata exhibited significantly lower permeability, suggesting increased tightness.

Boundary conditions were applied by imposing a variable pore water pressure distribution along the upstream face and lakebed, corresponding to the hydrostatic pressure exerted by the reservoir. Meanwhile, zero pore water pressure was prescribed along the downstream face, enabling the simulation to dynamically resolve the realistic flow path associated with steady-state conditions. Pore pressure evolution was monitored and recorded at two designated history points within the dam body, providing insight into internal hydraulic response and potential zones of elevated seepage pressure, Fig .15. In case of dam's model with varying properties, the recorded PWP reached magnitudes up to 91 Kpa at dam centre face and 62 Kpa at downstream face, while in case of dam's model with homogenous section, the recorded PWP reached magnitudes up to 52 Kpa at dam centre face and 38 Kpa at downstream face.

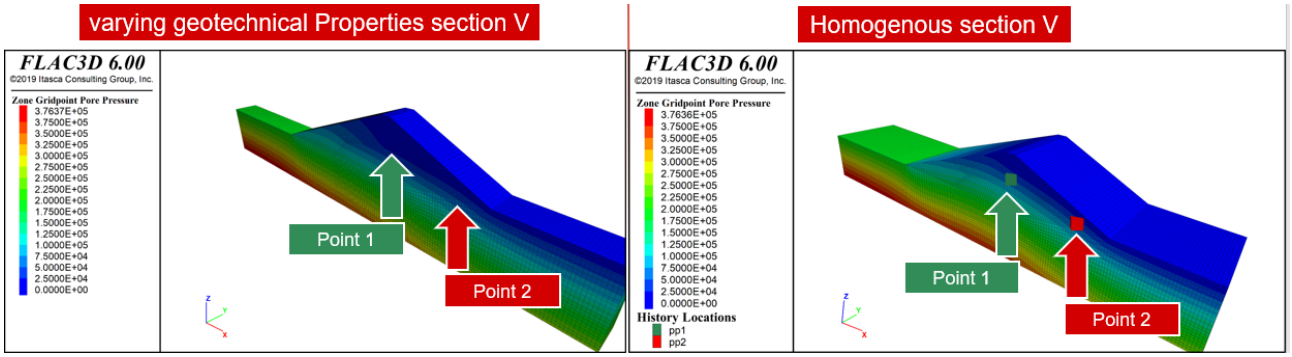

Fig (14) Pore pressure evolution in dam body

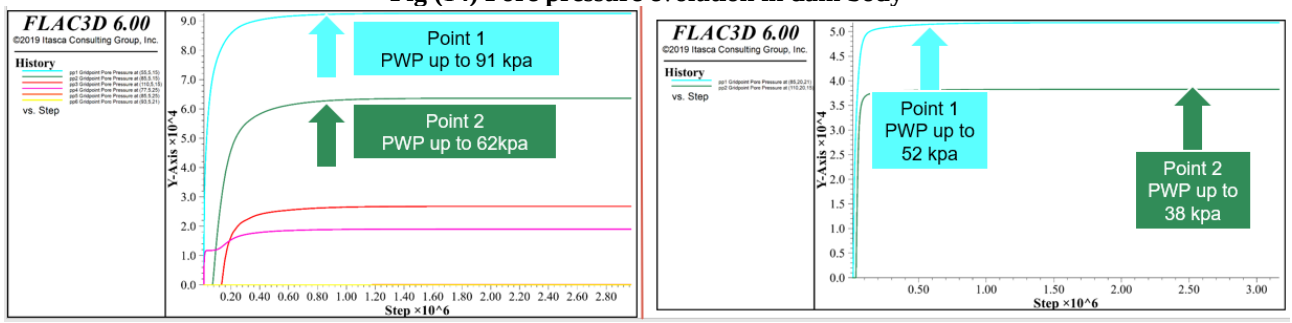

Fig (15) Pore pressure evolution in dam body, in both models.

Table (3) permeability properties

Group Name	Porosity	Permeability (m/s)
Dam Body		
body1	0.5207	3.27×10^{-9}
body2	0.4948	2.696×10^{-8}
body3	0.4948	2.696×10^{-8}
body4	0.4948	2.696×10^{-8}
body5	0.4948	2.696×10^{-8}
body6	0.4939	1.50×10^{-9}
body7	0.4137	2.01×10^{-9}
body8	0.4137	2.01×10^{-9}
Foundation		
foundation1	0.3000	1.00×10^{-10}
foundation2	0.4144	2.78×10^{-9}

By incorporating pore-water pressure in displacement analysis of dam's model of varying geotechnical properties, the recorded vertical settlements reached magnitudes up to 15 cm at upstream face and 11 cm at downstream face, while the horizontal displacements reached very big values indicating failure at upstream face, Fig .16.

http://journal.damascusuniversity.edu.sy/index.php/index/index

ISSN (online): 3031-085X

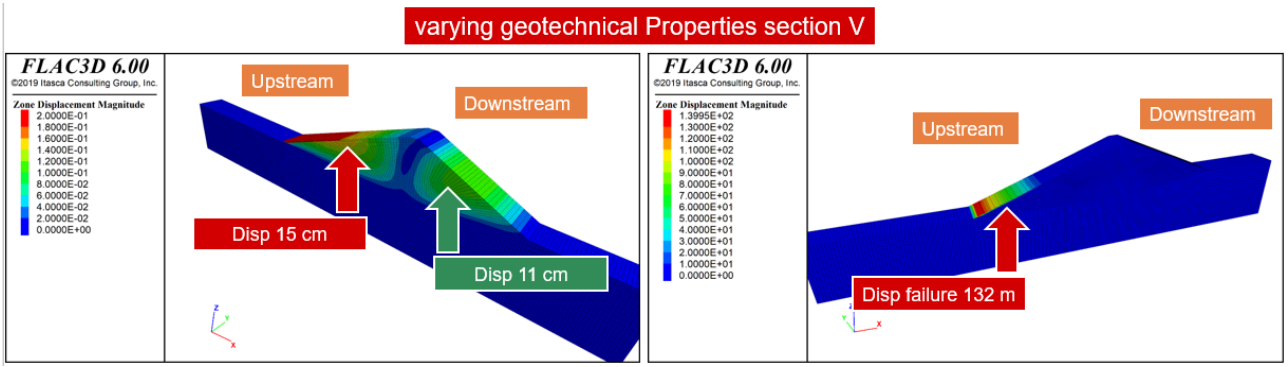

Fig (16) Displacements in dam body of varying geotechnical properties when incorporating pore-water pressure.

Validation of the 3D Model Against Actual Field Static Conditions

The analysis using Mohr-Coulomb and MCC constitutive models indicated significant sliding along the upstream toe of the dam, characterized by large displacements, and in the MCC analysis substantial displacements positioned spatially with the zone of observed failure along the upstream face in cross-sections with maximum dam height. In addition, the models did not reveal any signs of sliding on the downstream face, which is consistent with the real-world failure event that occurred in 2018 on the upstream side. However, Mohr-Coulomb constitutive model did not reflect the varying consolidation behavior and varying permeability coefficients that is proved by experimental assessment, that is emphasize the importance of choosing modified cam-clay model. That validate MCC constitutive model for analyzing dams with spatial geotechnical variability under static conditions, and make the base for future seismic analysis, Fig .17.

Dynamic Analysis of the 3D Dam Model:

The primary objective of the dynamic analysis was to evaluate boundary conditions and governing variables by simulating the response of a simplified three-dimensional model subjected to a seismic event. The Loma Prieta Earthquake (1989) record was selected for this purpose. This record is a well-documented, real-world motion that provides a realistic broadband frequency content, essential for exciting the diverse dynamic modes of a large, flexible earth fill dam and its foundation system.

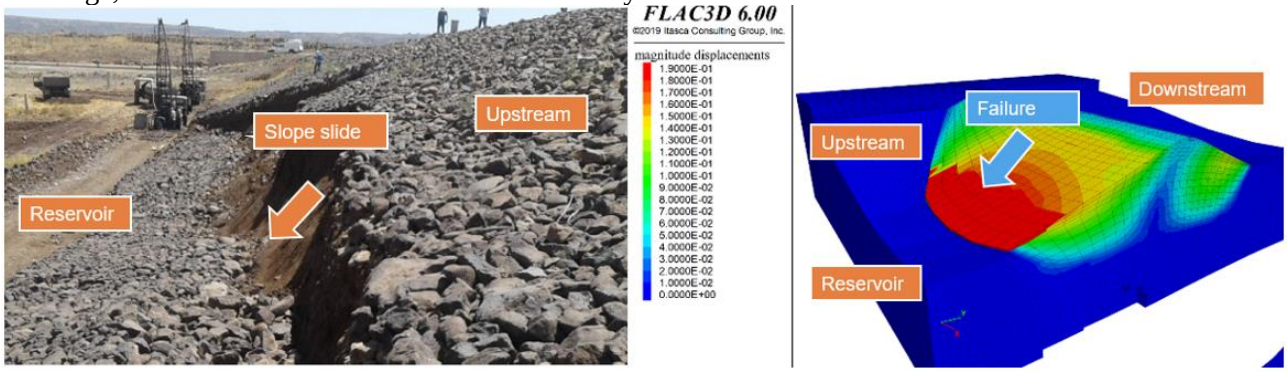

Fig (17) comparative assessment between the results of the analysis and the model

Its moderate peak ground acceleration (PGA) of approximately 0.11 g is suitable for a serviceability-level evaluation, allowing for the assessment of seismic performance and the development of deformations without inducing immediate collapse, which aligns with the initial phase of dynamic model validation. Furthermore, the record's significant duration of 40 seconds enables the observation of cumulative effects, such as pore

http://journal.damascusuniversity.edu.sy/index.php/index/index

ISSN (online): 3031-085X

pressure build-up and ratcheting displacements, while its dominant frequency of 2.47 Hz is within a range that can potentially interact with the fundamental period of typical embankment dams, making it a pertinent and widely referenced motion for seismic geotechnical analysis, Fig. 18. Boundary conditions of the Free-field type were implemented, to prevent wave reflection and ensure accurate simulation of outward energy dissipation, Seed et al [31]. The seismic input was applied at the base of the model, effectively mimicking the upward propagation of seismic waves through the underlying rock foundation. Results of this dynamic simulation were compared dam response when using Mohr-Coulomb or Modified Cam-Clay (MCC) constitutive models. Table 4 summarizes MCC properties of dam Body zones and foundations. Fig .19. showed that a distinctive behavior of the dam when using elastic or MCC model under seismic conditions. In the case of applying elastic constitutive model, dam failure occurs after 5 sec and acceleration is amplified 42 times from 0.009g at model base to 0.38g at dam crest, while in the case of applying MCC constitutive model, dam failure occurs after 1.88 sec and acceleration is amplified 3.7 times from 0.009g at model base to 0.034g at dam crest which is a more realistic scenario. Antoine et al [19]. by comparing displacements of both cases, in the case of applying elastic constitutive model, maximum displacements occur in horizontal direction toward downstream, at dam crest 3.5m, toe 7.8m, while at dam heel displacements were toward upstream by 0.8m. in the case of applying MCC constitutive model, displacements occur in horizontal direction toward downstream, at dam crest 0.65m, toe 1.2m, while at dam heel the maximum displacements occur toward upstream by 32m representing major failure of the upstream face, Gautham et al [17], which is the more realistic results taking into consideration static analysis and actual field conditions, Fig .20. as a result, Elastic model performance in seismic analysis failed to capture the actual behavior of the dam. The significant reduction in acceleration amplification observed with the Modified Cam-Clay (MCC) model, compared to the Mohr-Coulomb model, can be attributed to its fundamental ability to simulate energy dissipation through plastic deformation. While the Mohr-Coulomb model exhibits a primarily elastic-perfectly plastic response, the MCC model incorporates a hardening/softening yield surface and critical state soil mechanics principles. As seismic energy enters the dam, the MCC model allows for the development of progressive, irreversible plastic strains from the onset of cyclic loading. This intrinsic material damping mechanism effectively absorbs a portion of the input seismic energy, converting it into permanent deformations rather than amplifying it as elastic vibration. In contrast, the simpler Mohr-Coulomb model, without a hardening law, tends to transmit a greater proportion of the energy elastically until the sudden, global yield condition is met, leading to the unrealistically high acceleration amplification observed. Therefore, the MCC model provides a more physically realistic simulation of the dynamic energy absorption and inelastic material response of saturated or partially saturated earth fill materials under cyclic loading.

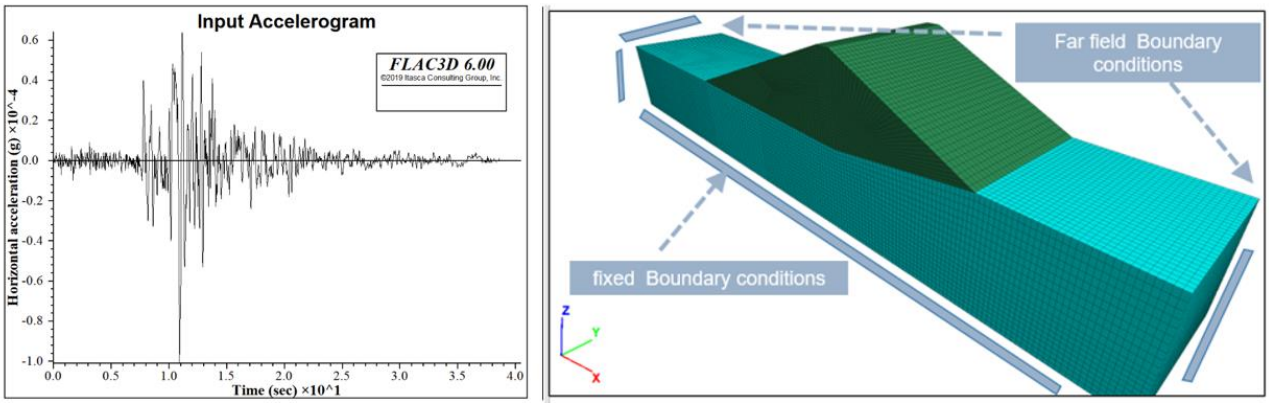

Fig (18) earthquake with a peak ground acceleration (PGA) of 0.11g, and boundary conditions.

Table (4) Modified Cam-Clay properties

Cc	e0	Compression Index (λ)	Cs	Swelling Index (κ)	Friction	friction - radians	critical State Slope (M)	Pre-consolidation pressure, kpa	P1	e1	e_{ref} at reference Pref	specific - volume - reference Vref
0.2292	0.49588	0.066617204	0.02371	0.006891435	26.18	0.456927198	1.034527165	440	130000	0.4682	0.952710504	1.952710504
0.22932	0.49665	0.066617204	0.02372	0.006891435	27.82	0.485550598	1.105343716	295	130000	0.47196	0.956722446	1.956722446
0.23752	0.47396	0.070062922	0.01168	0.003445717	25.52	0.445408025	1.006143191	295	99000	0.439322	0.913326984	1.913326984
0.24648	0.45787	0.073508639	0.03081	0.00918858	23.66	0.412944901	0.926562651	490	197000	0.4462	1.011742437	2.011742437
0.24083	0.46435	0.071504908	0.04139	0.012289906	23.66	0.412944901	0.926562651	410	98000	0.437259	0.916803475	1.916803475
0.37321	0.60902	0.100846316	0.05845	0.015795206	16.94	0.295658775	0.645426173	450	196000	0.44329	1.29877449	2.29877449
0.33432	0.57946	0.092028601	0.04715	0.012978392	25.52	0.445408025	1.006143191	392	161000	0.45942	1.197202066	2.197202066
0.31582	0.61639	0.084949478	0.04825	0.012978392	33.6	0.586430629	1.357123284	441	164000	0.55416	1.253642818	2.253642818

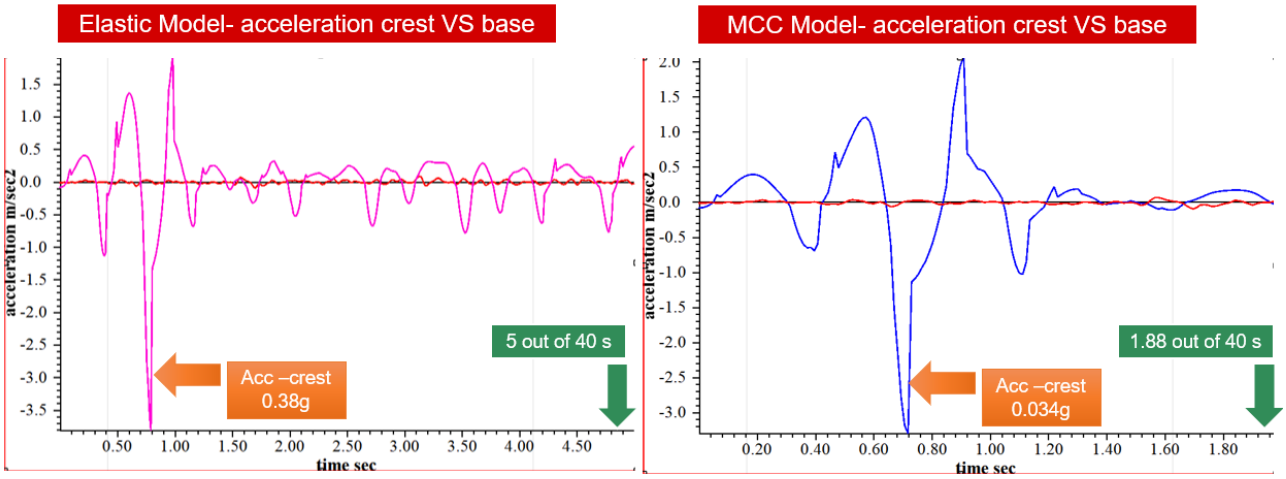

Fig (19) comparison of acceleration amplification at dam crest.

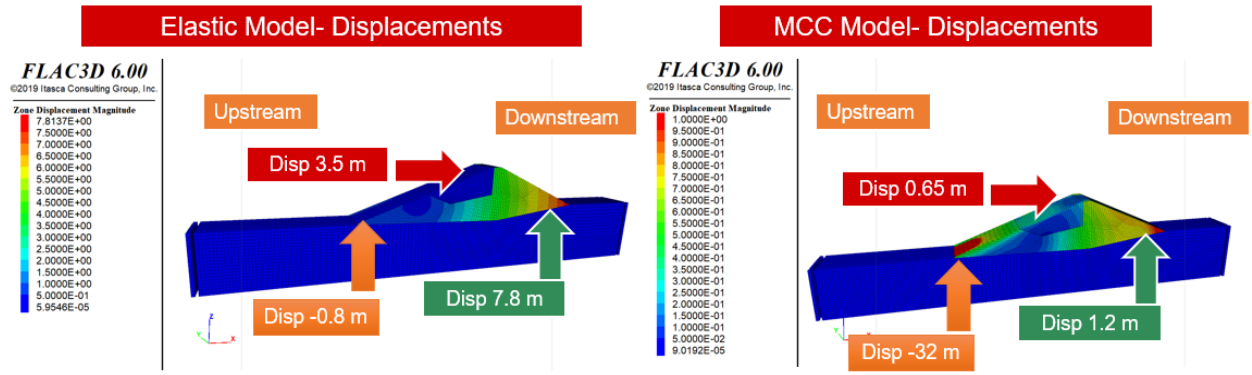

Fig (20) Comparison between displacements at the crest, toe anی heel of the dam, Elastic VS MCC models.

3. Conclusions

The findings of this research underscore the critical role of geotechnical irregularities in earth-fill dam embankments, particularly in regions with high seepage exposure and environmental fluctuations.

Under static situation and gravity loads, and in case of dam's model with varying properties, the recorded settlements reached magnitudes up to 14.4 cm at upstream face and 8.4 cm at downstream face, while in case of dam's model with homogenous section, the recorded settlements reached magnitudes up to 6.8 cm at upstream face and 5 cm at downstream face, Fig .13. accompanied by an increase in vertical stress in case of dam's model with varying properties, with peak values up to 500×103 Pa comparing to 92×103 Pa in case of dam's model with homogenous section. Under steady state seepage analysis, and in case of dam's model with varying properties, the recorded PWP reached magnitudes up to 91 Kpa at dam center face and 62 Kpa at downstream face, while in case of dam's model with homogenous section, the recorded PWP reached magnitudes up to 52 Kpa at dam center face and 38 Kpa at downstream face.

By incorporating pore-water pressure in displacement analysis of dam's model of varying geotechnical properties, the recorded vertical settlements reached magnitudes up to 15 cm at upstream face and 11 cm at downstream face, while the horizontal displacements reached very big values indicating failure at upstream face.

Under seismic conditions, and in the case of applying elastic constitutive model, dam failure occurs after 5 sec and acceleration is amplified 42 times from 0.009g at model base to 0.38g at dam crest, while in the case of applying MCC constitutive model, dam failure occurs after 1.88 sec and acceleration is amplified 3.7 times from 0.009g at model base to 0.034g at dam crest.

by comparing displacements of both cases, in the case of applying elastic constitutive model, maximum displacements occur in horizontal direction toward downstream, at dam crest 3.5m, toe 7.8m, while at dam heel displacements were toward upstream by 0.8m. in the case of applying MCC constitutive model, displacements occur in horizontal direction toward downstream, at dam crest 0.65m, toe 1.2m, while at dam heel the maximum displacements occur toward upstream by 32m. MCC model analysis results proved more realistic results taking into consideration static analysis and actual field conditions more than Elastic model, that failed to capture the actual behavior of the different zones of varying geotechnical properties of the dam under static and seismic conditions.

Funding: This Research is funded by Damascus University-Funder no (501100020595)

4. References:

1. Chakraborty, Sayantan et al. (2021). Geomaterial Characterization and Stability Assessment of Hydraulic Fill Dams. Journal of Materials in Civil Engineering, 33(2):04020446.DOI: https://doi.org/10.1061/(ASCE)MT.1943-5533.0003556
2. Mosadegh, Leila et al. (2020). Comparison of earthquake-induced pore water pressure and deformations in earthen dams using non-linear and equivalent linear analyses. Conference: Geo-Congress 2020.
3. Mosadegh, Leila et al. (2022). Effect of geomaterial variability on seismic response analyses of earthen dams. Engineering Geology 297:106513. DOI: https://doi.org/10.1016/j.enggeo.2022.106513
4. Aminfar, Mohamad Hossein et al. (2016). comparing the geodetical and geotechnical methods in investigating the deformation of earthfill dams; a case study of mahabad earth-fill dam, Iran. Journal of Engineering Science and Technology 11(7) :X-X.
5. Yang, Er-Jing et al. (2021). Analysis of Bound Water and Its Influence Factors in Mixed Clayey Soils. Journal of Water 2021 volume13.DOI: https://doi.org/10.3390/w13131760
6. Khaled Chowdhury et al. (2019). Lessons Learned from Re-Evaluation of the Upper and Lower San Fernando Dams Using Current State of Practice in Numerical Modelling. Conference: 2019 USSD Conference and Exhibition At: Chicago, IL.
7. Majeed, Qutaiba. (2015). Flow and Deformation Analysis of Zoned Earth Dam by the Finite Element Method. Diyala Journal of Engineering Sciences 8(3):38-62.
8. Sánchez-Martín, José et al. (2020). Optimized Design of Earth Dams: Analysis of Zoning and Heterogeneous Material in Its Core. Sustainability 12(16):6667.DOI: https://doi.org/10.3390/su12166667
9. Pardoen, Benoît et al. (2019). Numerical Modelling of Zoned Rockfill Dam during Construction Considering Granular Interface Behaviour. Journal of Geotechnical and Geo-environmental Engineering145(3).DOI: https://doi.org/10.1061/(ASCE)GT.1943-5606.0002007
10. Gordan, Behrouz et al. (2022). Review on Dynamic Behaviour of Earth Dam and Embankment During an Earthquake. Geotechnical and Geological Engineering volume 40, pages3–33 (2022). DOI: https://doi.org/10.1007/s10706-021-01938-1
11. Ambarakonda, Pooja et al. (2017). A Comparison Between Linear and Nonlinear Seismic Behaviour of Earth Dam on Layered Soil. Conference: 6th Indian Young Geotechnical Engineers Conference.
12. Moghadam, S Abdolreza. et al. (2020). Seismic finite element analysis of non-homogeneous embankment located in asymmetric valley. Innovative Infrastructure Solutions 5(3). DOI:
13. https://doi.org/10.1007/s41062-020-0267-3
14. Wang, Yuke et al. (2020). Stiffness degradation of natural soft foundation in embankment dam under complex stress paths with considering different initial states. Applied Ocean Research 104(4):1-22.DOI: https://doi.org/10.1016/j.apor.2020.102385
15. Ambarakonda, Pooja et al. (2017). Parametric Study on Deformation Behaviour of Earth Dam on Multi Layered Soil Deposits under Seismic Loading. Conference: Indian Geotechnical Conference-2017.
16. Lizarraga, Sanchez, H. et al. (2012). Effect of Spatial Variability of Soil Properties on the Seismic Response of Earth Dams. 15 WCEE LISBOA 2012.
17. Sanchez, Heidy H. (2014). Effects of spatial variability of soil properties on the seismic response of an embankment dam. Soil Dynamics and Earthquake Engineering 64(64):113–128. DOI: https://doi.org/10.1016/j.soildyn.2014.04.015
18. Gautham, Adapa et al. (2020). Seismic stability of embankments with different densities and upstream conditions related to the water level. Soils and Foundations -Tokyo- 61(1). DOI: https://doi.org/10.1016/j.sandf.2020.07.001
19. Zhongzhi, Fu. (2020). Heightening of an Existing Embankment Dam: Results from Numerical Simulations. In book: Dam Engineering.

20. Antoine, Duttine et al. (2019). Effects of compaction on soil undrained shear strength deteriorating during undrained cyclic loading and controlling seismic stability of embankment. E3S Web of Conferences 92:18003. DOI: https://doi.org/10.1051/e3sconf/20199218003
21. Ono, Keisuke et al. (2011). Possible earthen dam failure mechanisms of Fujinuma reservoir due to the Great East Japan Earthquake of 2011. Hydrological Research Letters 5:69-72. DOI: https://doi.org/10.3178/hrl.5.69
22. Ji, Enyue et al. (2018). Numerical Simulation of Hydraulic Fracturing in Earth and Rockfill Dam Using Extended Finite Element Method. Advances in Civil Engineering 2018(2):1-8. DOI: https://doi.org/10.1155/2018/2123038
23. Secchi, Stefano. (2012). A method for 3-D hydraulic fracturing simulation. International Journal of Fracture 178(1-2). DOI: https://doi.org/10.1007/s10704-012-9758-3
24. Talukdar, Priyanka et al. (2021). Finite element analysis for identifying locations of cracking and hydraulic fracturing in homogeneous earthen dams. International Journal of Geo-Engineering 12(1). DOI: https://doi.org/10.1186/s40703-021-00139-2
25. Caballero, et al. (2022). Geotechnical Visualization and Three-Dimensional Geostatistics Modeling of Highly Variable Soils of a Hydraulic Fill Dam. dams. Journal of Geotechnical and Geoenvironmental Engineering volume 148(11).DOI: https://doi.org/10.1061/(ASCE)GT.1943-5606.0002872
26. Guo, P et al, (2024). Investigation on elastic–plastic deformation and mechanical failure of varied-moisture expansive soil subjected to dry–wet cycles. Journal of Environmental Earth Sciences volume 83(14). DOI: https://doi.org/10.1007/s12665-024-11634-x
27. Horikoshi, K et al. (2015). Suffusion-induced change in spatial distribution of fine fractions in embankment subjected to seepage flow. Journal of Soils and Foundations volume 55 issue 5. DOI: https://doi.org/10.1016/j.sandf.2015.09.015
28. Khan, F.S. & Malik, A.A. (2013). Probability and Sensitivity Analysis of the Slope Stability of Naulong Dam. Journal of Pak. J. Engg. & Appl. Sci volume 13 (p. 54-64).
29. Seequent. (2024). Sensitivity analysis. In book: Stability Modeling with GEOSTUDIO (pp.129-130).
30. Hardin, B. O., and V. P. Drnevich. "Shear Modulus and Damping in Soils: I. Measurement and Parameter Effects, II. Design Equations and Curves," Technical Reports UKY 27-70-CE 2 and 3, College of Engineering, University of Kentucky, Lexington, Kentucky. [These reports were later published in the Journal of Soil Mechanics and Foundation Division, ASCE, Vol. 98, No. 6, pp. 603-624 and No. 7, pp. 667-691, in June and July 1972.]
31. Idriss, I. M., and Joseph I. Sun. User's Manual for SHAKE-91. University of California, Davis, Centre for Geotechnical Modeling, Department of Civil & Environmental Engineering (November 1992).
32. Seed, H. Bolton, and I. M. Idriss. "Soil Moduli and Damping Factors for Dynamic Response Analysis," Earthquake Engineering Research Centre, University of California, Berkeley, Report No. UCB/EERC-70/10, p. 48 (December 1970).
33. Seed, H. Bolton, et al. "Moduli and Damping Factors for Dynamic Analyses of Cohesionless Soils," Journal of the Geotechnical Engineering Division, ASCE, Vol. 112, No. GT11, pp. 1016-1032 (November 1986). DOI: https://doi.org/10.1061/(ASCE)0733-9410(1986)112:11(1016)
34. Sun, J. I., R. Golesorkhi and H. Bolton Seed. "Dynamic Moduli and Damping Ratios for Cohesive Soils," Earthquake Engineering Research Centre, University of California, Berkeley, Report No. UCB/EERC-88/15, p. 42 (1988).
35. Vucetic, M., and R. Dobry. "Effect of Soil Plasticity on Cyclic Response," in J. Geotech. Eng. Div., ASCE, Vol. 111, No. 1, pp. 89-107 (January 1991). DOI: https://doi.org/10.1061/(ASCE)0733-9410(1991)117:1(89)
36. AL-ARAB, et al, (2024). Comparison of Adaptive and non-Adaptive Nonlinear Static Analysis Methods for Estimating Seismic Demand. Journal of Earthquake and Disaster Research Vo 1 number (2) -2222: 22-22
37. Al Hariri et al, (2025). Soil-Structure Interaction Effect on Seismic Response Modification Coefficient of Dual System Using Substructure Approach. Journal of Earthquake and Disaster Research Vo 1 number (1) -2025: 1-15

38. Itasca Consulting Group, Inc. FLAC3D — Fast Lagrangian Analysis of Continua in Three Dimensions, Theory and Background. 6th ed., Itasca Consulting Group, Inc., Minneapolis, MN (2021).